

A conserved splicing mechanism of the *LMNA* gene controls premature aging

Isabel C. Lopez-Mejia¹, Valentin Vautrot², Marion De Toledo¹, Isabelle Behm-Ansmant², Cyril F. Bourgeois³, Claire L. Navarro⁵, Fernando G. Osorio⁴, José M. P. Freije⁴, James Stévenin³, Annachiara De Sandre-Giovannoli⁵, Carlos Lopez-Otin⁴, Nicolas Lévy⁵, Christiane Branlant² and Jamal Tazi^{1,*}

¹CNRS, UMR 5535, University of Montpellier, Institut de Génétique Moléculaire de Montpellier, 1919 Route de Mende, Montpellier 34293, France, ²CNRS UMR 7567, Biopôle, Faculté de médecine, Université Henri Poincaré-Nancy I, 9 Avenue de la Forêt de Haye, 54506 Vandoeuvre-les-Nancy, France, ³IGBMC Department of Functional Genomics and Cancer, CNRS UMR 7104, INSERM U 964, University of Strasbourg, 1 Rue Laurent Fries, 67404 Illkirch Cedex, France, ⁴Departamento de Bioquímica y Biología Molecular, Facultad de Medicina, Instituto Universitario de Oncología, Universidad de Oviedo, 33006-Oviedo, Spain and ⁵INSERM UMR_S910, Faculté de Médecine, Université de la Méditerranée, Boulevard Jean Moulin, 13385 Marseille Cedex 05, France

Received June 28, 2011; Revised August 12, 2011; Accepted August 24, 2011

Hutchinson–Gilford progeria syndrome (HGPS) is a rare genetic disorder phenotypically characterized by many features of premature aging. Most cases of HGPS are due to a heterozygous silent mutation (c.1824C>T; p.Gly608Gly) that enhances the use of an internal 5' splice site (5'SS) in exon 11 of the *LMNA* pre-mRNA and leads to the production of a truncated protein (progerin) with a dominant negative effect. Here we show that HGPS mutation changes the accessibility of the 5'SS of *LMNA* exon 11 which is sequestered in a conserved RNA structure. Our results also reveal a regulatory role of a subset of serine–arginine (SR)-rich proteins, including serine–arginine rich splicing factor 1 (SRSF1) and SRSF6, on utilization of the 5'SS leading to lamin A or progerin production and a modulation of this regulation in the presence of the c.1824C>T mutation is shown directly on HGPS patient cells. Mutant mice carrying the equivalent mutation in the *LMNA* gene (c.1827C>T) also accumulate progerin and phenocopy the main cellular alterations and clinical defects of HGPS patients. RNAi-induced depletion of SRSF1 in the HGPS-like mouse embryonic fibroblasts (MEFs) allowed progerin reduction and dysmorphic nuclei phenotype correction, whereas SRSF6 depletion aggravated the HGPS-like MEF's phenotype. We demonstrate that changes in the splicing ratio between lamin A and progerin are key factors for lifespan since heterozygous mice harboring the mutation lived longer than homozygous littermates but less than the wild-type. Genetic and biochemical data together favor the view that physiological progerin production is under tight control of a conserved splicing mechanism to avoid precocious aging.

INTRODUCTION

Different proteins are produced by alternative splicing and or polyadenylation of the *LMNA* gene, including lamin A, lamin C and progerin (Fig. 1A) (1–5). Lamin A and lamin C are major components of the nuclear lamina, a complex molecular interface located between the inner membrane of the nuclear

envelope and chromatin (6). Lamins A and C are also distributed throughout the nucleoplasm and are involved in crucial functions, including DNA replication, transcription, chromatin organization, nuclear positioning and shape, as well as the assembly/disassembly of the nucleus during cell division (6–8).

Hutchinson–Gilford progeria syndrome (HGPS) is a dominant disease usually caused by heterozygous *de novo* mutations in the

*To whom correspondence should be addressed at: IGMM-CNRS, 1919 Route de Mende, 34293 Montpellier. Tel: +33 34359685; Fax: +33 34359634; Email: jamal.tazi@igmm.cnrs.fr

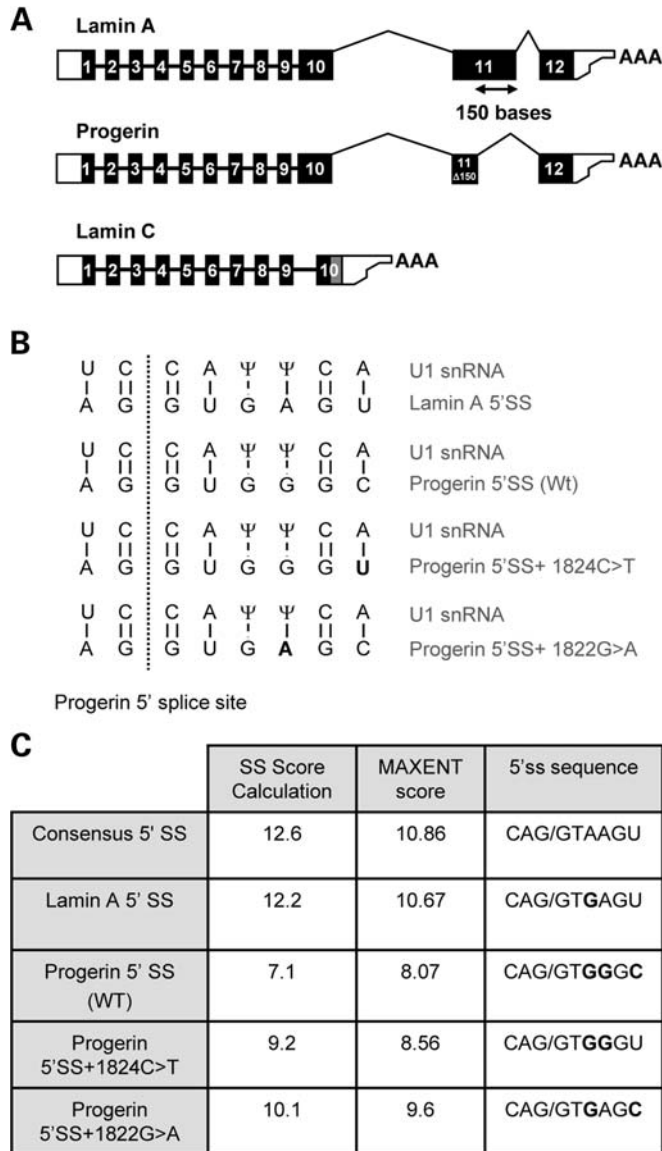


Figure 1. LMNA isoforms and properties of the progerin and lamin 5'SSs. (A) Three different proteins are produced from the *LMNA* gene. Cartoon showing the exon structure of the three different forms of *LMNA* mRNA showing the position of the alternative splice site used in progerin and alternative polyadenylation site that is specific for lamin C. Exons are numbered and shown as boxes (coding regions are solid). Introns are shown as lines. The site of the HGPS mutation is shown in bold. (B) The HGPS progeria mutations increase complementarity of the progerin splice site for U1 snRNA. The wild type and mutant progerin 5'SSs are shown base paired to U1 snRNA sequence. The mutation creates an AU base pair at the plus 6 position shown in bold. (C) Predicted bioinformatic scores of the *LMNA* splice sites. Bioinformatic scores for a consensus splice site (consensus 5'SS), lamin A 5'SS, the progerin 5'SS and the mutants c.1824C>T and c.1822G>A progerin 5'SS are shown using two different programs. Note the near-perfect score of the lamin 5'SS and the moderate improvement in the mutated progerin 5'SS+ 1824C>T compared with WT progerin 5'SS.

LMNA gene that leads to accumulation of a truncated protein, commonly called progerin (4,5). Progerin is hardly detectable in wild-type (WT) cells but a single nucleotide substitution c.1824C>T, recurrent in the majority of typical HGPS patients, promotes activation of a 5' splice site (5'SS) in exon 11, causing a large increase

in the levels of transcripts encoding progerin compared with the other *LMNA* isoforms. Due to a 150 nucleotides deletion from exon 11, progerin retains the C-terminal CAAX box of lamin A (encoded by exon 12), which undergoes methyl esterification and farnesylation, but it lacks 50 internal amino acids essential for a specific cleavage step involved in lamin A maturation (4–11). Progerin is therefore permanently farnesylated and carboxymethylated (12,13) which leads to its abnormal anchoring to the nuclear membrane throughout the cell cycle (13,14). The production of progerin interferes with the integrity of the nuclear lamina, causing misshapen nuclei, and also adversely affects other important cellular processes, such as interphase chromatin, mitosis and cell proliferation (4,5,10,11,14). The finding that progerin is expressed at detectable levels in healthy individuals and seems to accumulate with age has led to the proposal that progerin could be involved in physiological aging (10,15–17). However, to date very little is known about the underlying splicing mechanism leading to usage of the internal 5'SS in exon 11 and how this selection might alter lifespan.

Major players in both splice-site recognition and intron excision are five small nuclear RNAs (U1, U2, U4, U5 and U6) which have dynamic specific interactions via base pairing with the pre-mRNA (18), and notable among these are the base pairing between U1 snRNA and the 5'SS. However, the information contained in the nucleotide sequence in splice sites is not sufficient for regulation and it has been shown that the RNA–protein complexes which form on the pre-mRNA also help the recognition of exons (19). The majority of splicing regulatory proteins in these complexes belongs to the heterogeneous ribonucleoprotein (hnRNP) and serine–arginine (SR)-protein families. hnRNPs were initially defined as the major proteins binding to RNA polymerase II transcripts in the course of transcription. SR proteins containing arginine–serine rich domains play essential roles in the splicing reaction (19–22). hnRNPs and SR proteins contain both RNA-binding and protein–protein interaction domains. They bind with low specificity to accessible parts of the pre-mRNA and RNA secondary structures strongly influence their binding efficiency (23–27).

Here we use *in vitro* and *in vivo* approaches to explore the sharp differences in splice-site usage in progeria patients. By probing the conserved structure of the alternatively spliced RNA as well as the proteins that bind to it, we demonstrate that the c.1824C>T mutation increases the accessibility of the exon 11 internal 5'SS which should facilitate U1 snRNP binding and discover a previously undescribed repression by the SR protein serine–arginine rich splicing factor 6 (SRSF6), whereas SRSF1 has an opposite action. Thus RNA-binding proteins and RNA structure should cooperate with enhanced U1 complementarity in the regulation of production of the progerin. Additionally, mouse embryonic fibroblasts (MEFs) that harbor a synonymous C>T (GGC>GGT, Gly609Gly) single-base substitution of the mouse *Lmna* gene demonstrate that this splicing mechanism is conserved from the mouse to human and is determinant in the control of lifespan.

RESULTS

Conserved RNA structure at the progerin 5'SS

The synonymous c.1824 C>T (GGC>GGT, G608G) single-base substitution in exon 11 of the *LMNA* gene that potentiates

usage of the exonic 5'SS (hereafter referred to as the progerin 5'SS) is not expected to have a strong effect on splicing because it occurs at the final, highly variable (+6) position of the 5'SS consensus (25,26,28–30). Furthermore, computational analyses to score the strength of either the WT or the mutated (c.1824C>T) form of the progerin 5'SS in comparison with the downstream 'authentic' 5'SS that is used to produce lamin A (hereafter referred to as the lamin A 5'SS) revealed that the scores of the progerin 5'SS are lower than the lamin A 5'SS (Fig. 1A–C). While the c.1824C>T mutation augments the score of the progerin 5'SS, it is not sufficient to make it comparable to the lamin A 5'SS which has a close to perfect score (Fig. 1B and C). However, the mutation results in the production of more progerin mRNA than lamin A mRNA (see below), suggesting that the mutation likely enhances recognition of the progerin 5'SS by other mechanisms than simply by enhancing base pairing with U1 snRNP. Given the fact that RNA structure may be essential for the interaction of a target pre-mRNA and spliceosomal components, and thereby may influence splice-site selection (20,31,32), we decided to assay for disruption or occurrence of RNA structures surrounding the c.1824C>T mutation in exon 11 of the *LMNA* gene. To this end, radiolabelled RNAs were transcribed, denatured and refolded and then digested with different ribonucleases specific either for accessible single-stranded regions (T1 and T2 RNases) or for double-stranded or stacked RNA regions (V1 RNase). To avoid border effects, the sites of cleavage were analyzed by primer extension on a series of overlapping fragments of different sizes. The most stable secondary structure that fits the best with the experimental data was predicted with the M-fold software by introducing experimental data as constraints. In all RNA fragments studied, the segment from positions 1804–1851, which contains the progerin 5'SS was always folded into a compact 2-D structure (Fig. 2A) with the progerin 5'SS located in the stem. This part of stem-loop (SL) structure IV will now be denoted as the progerin stem-loop (progerin SL). Its terminal tetra-loop is expected to be structured because of its limited accessibility to RNases. In contrast, the lamin A 5'SS was found to be located in a highly accessible single-stranded region in all the RNA fragments studied (Fig. 2A and Supplementary Material, Fig. S1). Thus, in contrast to the lamin A 5'SS, recognition of the progerin 5'SS in the WT gene is normally disfavored due to its sequestration in a structured region.

Interestingly, when repeating the experiment on transcripts containing the c.1824C>U mutation, we found that the progeria mutation induces some opening of the progerin SL terminal loop which flanks the progerin 5'SS, as shown by the strong accessibility to T1 RNase (Fig. 2B, right panel). Although the mutation is not expected to affect the base pairing of the stem structure, the stability of the terminal G-C pair may be also slightly decreased based on the appearance of some T2 RNase cleavage 3' to residue C1828 (Fig. 2B, right panel). The overall conformational change of the progerin SL might therefore increase the accessibility of the progerin 5'SS to U1 snRNA and explain, at least in part, the increased usage of this site in HGPS.

To further analyze the unexpected accessibility of the loop of the progerin SL after the c.1824C>U mutation, we decided to assess two novel mutations, one located in the stem and

expected to alter RNA structure of the region and a second in the loop of the progerin SL, as the original mutation. The first is a HGPS mutation, which significantly increased the complementarity of the progerin 5'SS with U1 snRNA (Fig. 1), and was also found to increase utilization of the progerin 5'SS (4,5). By probing the structure of the mutated pre-mRNA region with T1 and T2 RNases, we observed an opening of the terminal loop in the progerin SL (Supplementary Material, Fig. S2a). The G>A mutation disrupts a G–C base pair close to the WT terminal loop and as a consequence several G residues are cleaved by T1 RNase within the opened terminal loop. A better accessibility of the 5'SS region, together with an increased complementarity to the U1 snRNA, may explain the strong utilization of the progerin 5'SS in the β -globin-LMNA reporter RNA incubated in HeLa nuclear extract (see below and Supplementary Material, Fig. S2b).

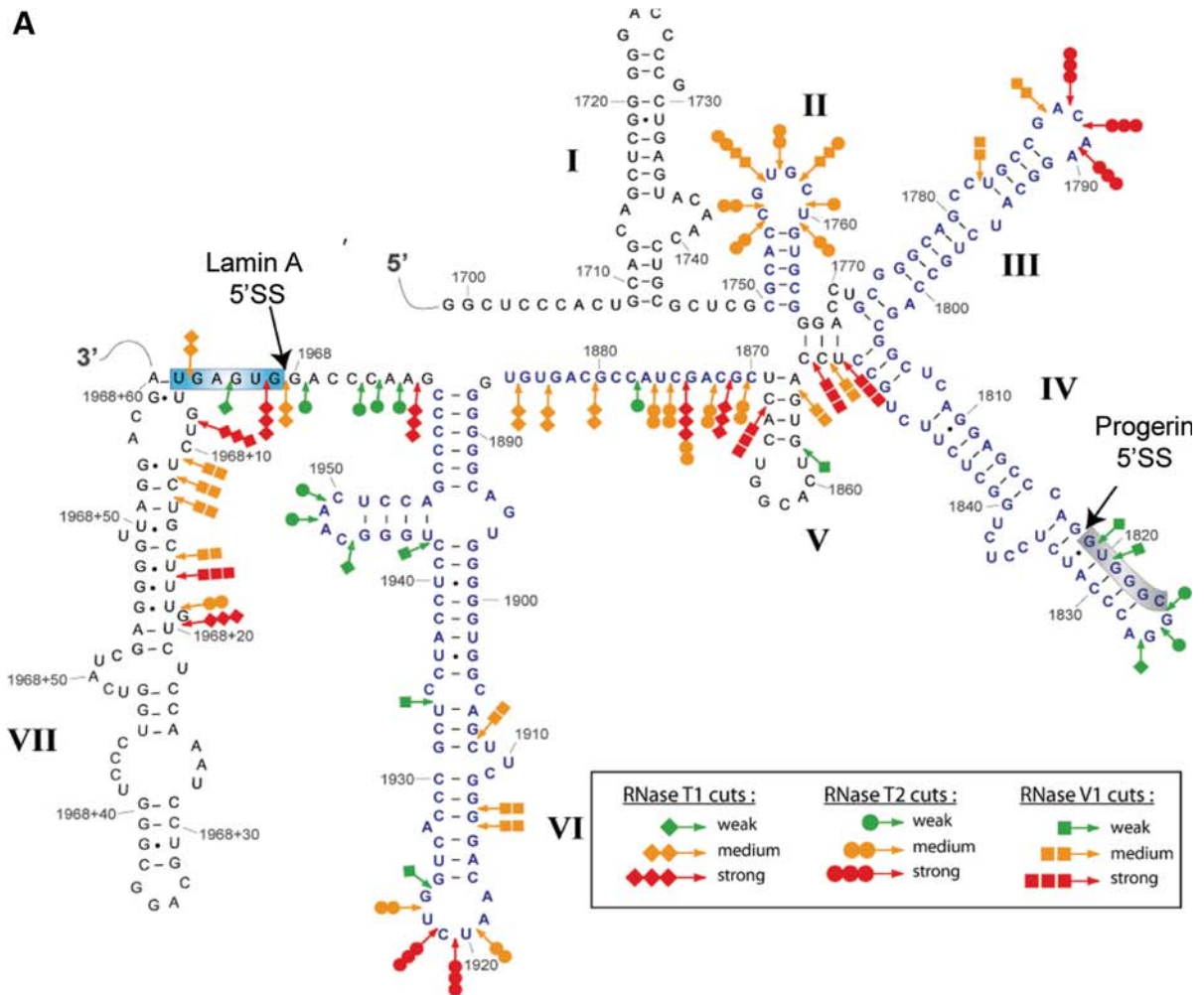
For the second mutation, we replaced the first residue of the loop, residue G1825 which is located 3' to the U1 binding site into an A residue and tested for the effect on both RNA structure and utilization of the progerin 5'SS (Supplementary Material, Fig. S2a and b). Interestingly, this mutation increased both the accessibility of the loop to RNases (especially RNase T2) and the utilization of the progerin 5'SS (Supplementary Material, Fig. S2a and b). Altogether with the mutation c.1824C>U data, these data show a possible correlation between the accessibility of the terminal loop of the progerin SL and the efficiency of the progerin 5'SS utilization.

Recognition of the progerin 5'SS by the SR proteins SRSF1 and SRSF6

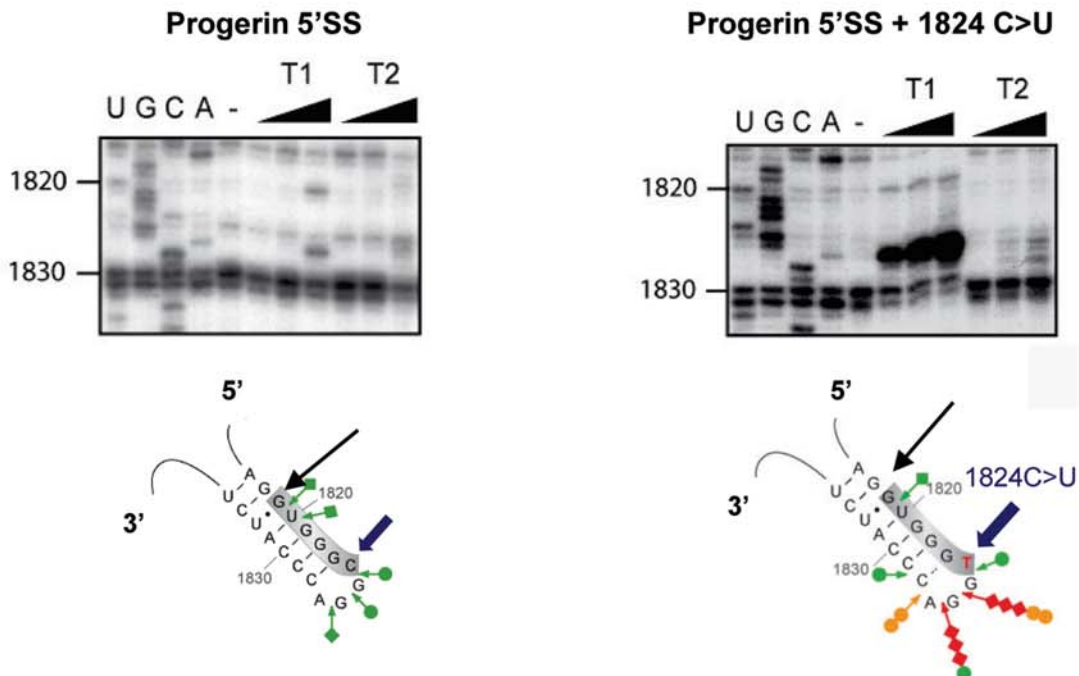
Mutations responsible for splicing defects at the origin of human diseases are either found in splice sites, or in regulatory sequences involved in the control of splicing (25,28,33–35). Therefore, we used various approaches to investigate whether the c.1824C>T mutation might modify the binding of some splicing regulatory factors at or in the vicinity of the progerin 5'SS, in addition to its effect on the RNA structure.

First, we identified nuclear proteins able to bind to the progerin SL structure by fusing three MS2 coat protein RNA-binding sites at the 3' extremity of the progerin SL RNA (Supplementary Material, Fig. S3a) and purifying the complexes formed by incubation of the tagged RNA in HeLa nuclear extract. The complexes were affinity purified using an MS2 coat protein fused to the Maltose Binding Protein bound to amylose beads, as previously described (36,37). Both mass spectrometry analysis of protein bands purified from sodium dodecyl sulfate polyacrylamide gel electrophoresis (SDS–PAGE) and western blot analysis (Supplementary Material, Fig. S3b) of the bound proteins revealed the presence of the SR proteins SRSF1 and SRSF6. The association of both proteins was also observed when using a longer RNA called progerin ESL (Extended Stem Loop) which contains stem loops III, IV and V in addition to progerin SL, and association of SRSF6 was stronger with this longer RNA (see Fig. 1 and Supplementary Material, Fig. S3a). Interestingly, experiments done with SL or ESL RNAs containing the c.1824 C>U mutation revealed that SRSF1 association with each of the mutated progerin SL and ESL RNAs was strongly diminished,

A



B



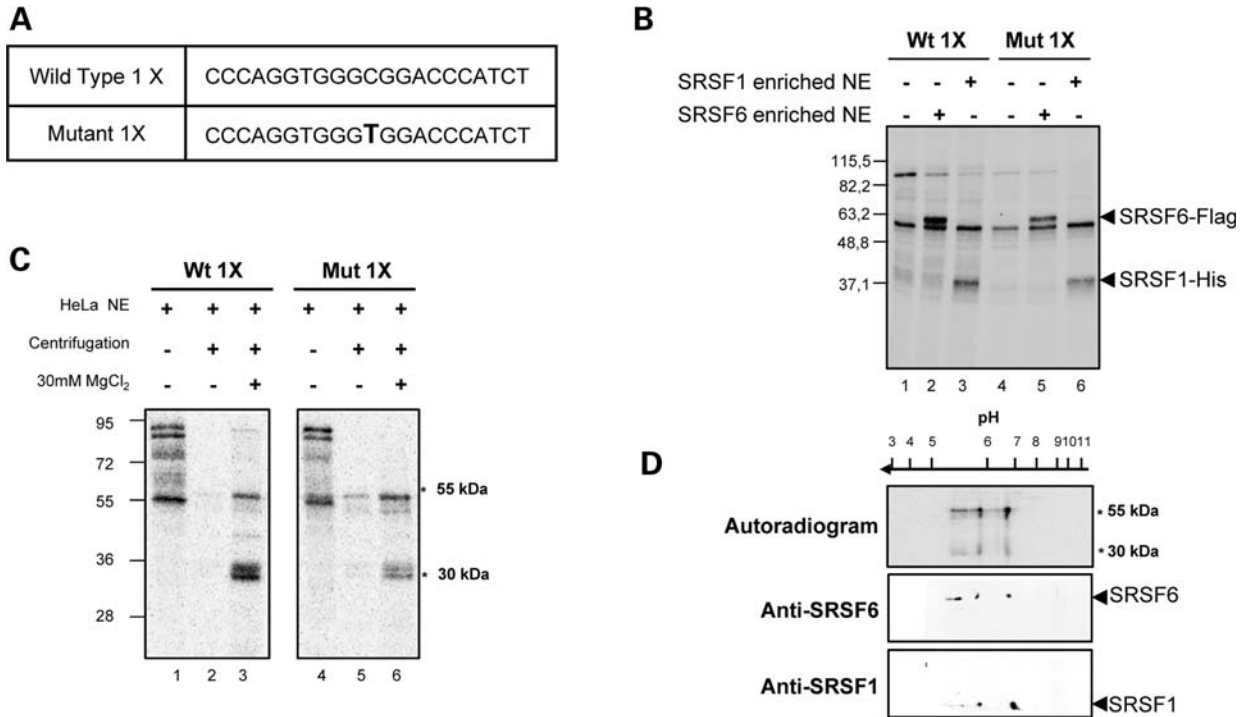


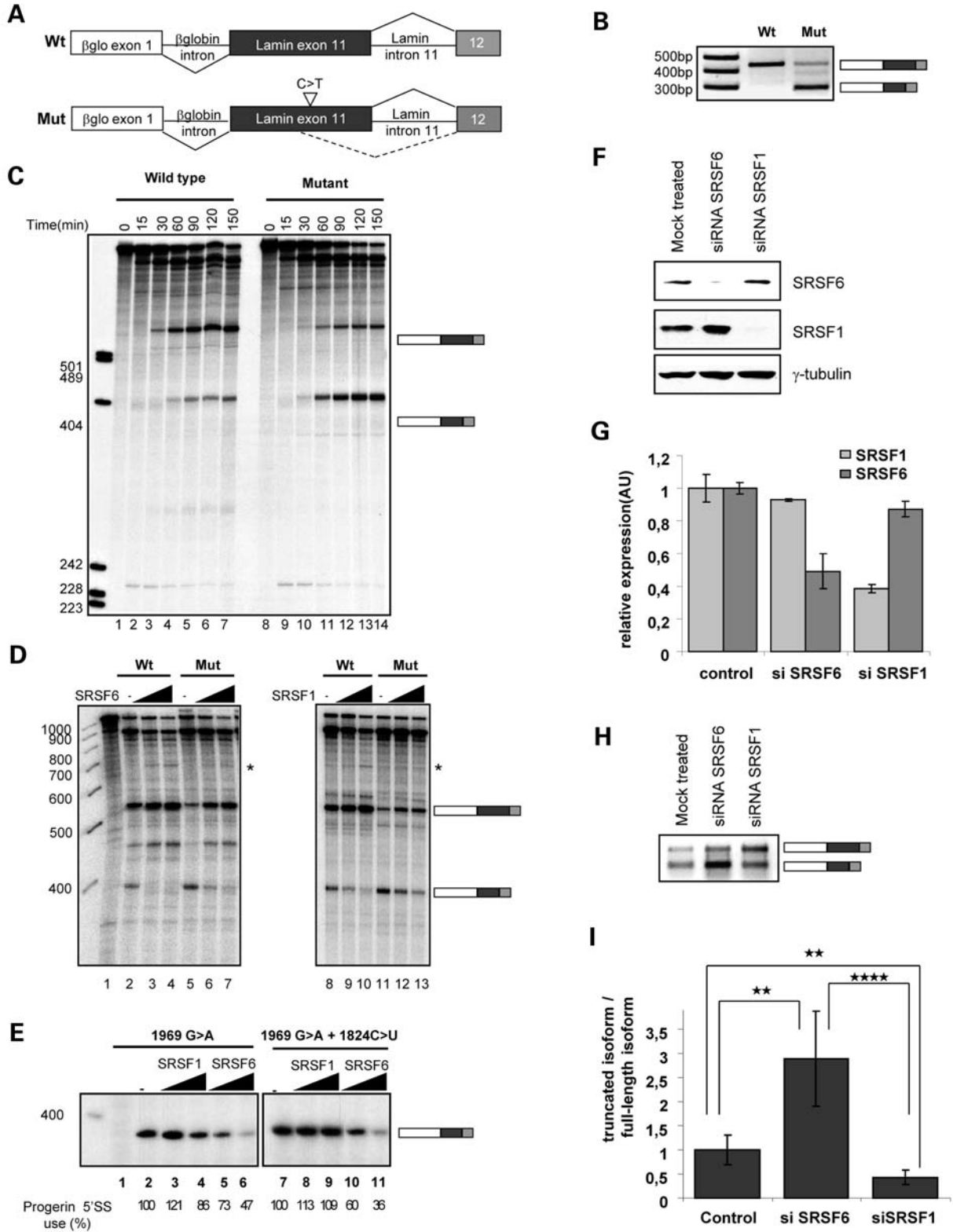
Figure 3. The SR proteins SRSF1 and SRSF6 cross-link to the WT and the c.1824C>U mutant progerin SL. (A) Sequences of the RNA constructs used for cross-linking in nuclear extracts. The sequences shown were embedded within a 40 mer RNA with invariable flanking sequences. The different RNA probes comprise monomers (1X) of the progerin 5'SS contained in the SL structure in the wild-type (WT 1X) or mutated versions (Mut 1X). (B) Cross-linking assay in nuclear extract of untransfected cells (lanes 1 and 4) or transfected cells expressing flag-tagged SRSF6 (lanes 2 and 5) or His-tagged SRSF1 (lanes 3 and 6). The constructs (detailed in A) were cross-linked in different nuclear extracts and after RNase cleavage bound proteins were separated by SDS-PAGE and visualized by autoradiography. The size of the protein markers is shown on the left. (C) The cross-linking experiment (detailed in B) was repeated but with HeLa nuclear extract (HeLa NE, lanes 1 and 4) or with supernatant of HeLa nuclear extract treated with 30 mM MgCl₂ and centrifugation (lanes 2 and 5) or with the 30 mM MgCl₂ precipitation-enriched nuclear extract (lanes 3 and 6). (D) 2D gel analysis of UV-cross-links using the mutated version of the progerin SL probe and HeLa nuclear fraction that precipitates at 30 mM MgCl₂. This gel was transferred to a nitrocellulose membrane and submitted to autoradiography and then probed with antibodies specific for SRSF6 and SRSF1.

whereas association of SRSF6 with the SL RNA was diminished to a lower degree, but its association with the ESL RNA was also more extensively reduced (Supplementary Material, Fig. S3b). Altogether, this revealed another property of the mutated RNA which may influence progerin 5'SS utilization. However, based on gel shift experiments performed with recombinant SRSF1 and an *in vitro* transcribed progerin SL structure, the affinity of the isolated protein SRSF1 for the WT RNA is low, suggesting that its association in the extract is mediated or reinforced by the presence of some other proteins (Supplementary Material, Fig. S3c).

Therefore, to identify proteins that bind directly to the segment containing the progerin 5'SS, we performed UV cross-linking experiments using ³²P-labeled RNA probes. Probe WT of 21 nucleotides contains the progerin 5'SS and corresponded

to the upper part of the progerin SL (Figs 2A and 3A). The mutated probe (Mut) included the c.1824C>T mutation. Probes were cross-linked in 293E and HeLa cells nuclear extracts, or in nuclear extract fraction precipitated with magnesium which is one of the steps used in SR protein purification (38). Labeled proteins were analyzed by electrophoresis on SDS-polyacrylamide gels after RNase treatment and visualized by autoradiography. Using whole nuclear extracts, WT probe predominantly cross-linked to proteins with apparent molecular weights of 30, 55 and 120 kDa, whereas only 55 and 120 kDa protein bands are revealed with the Mut progerin probe (Fig. 3B, lanes 1 and 4). However, only two main bands at 55 and 30 kDa were detected when UV-cross-linking was performed with the MgCl₂-enriched SR protein fraction (Fig. 3C, lanes 3 and 6). According to their electrophoretic mobility, the

Figure 2. Secondary structure around LMNA exon 11 splice sites. (A) The secondary structure model proposed for exon 11 and part of intron 11 of the human LMNA pre-mRNA. The model is proposed based on thermodynamic considerations and on the results of enzymatic digestions shown in Supplementary Material, Figure S1. V1, T1 and T2 RNase cleavages are represented by arrows surmounted by squares, dots and diamonds, respectively. Red, orange and green symbols indicate a high, medium or low extent of cleavage, respectively. The structure representation shows all the bases used and the position of the splice sites are indicated with arrows. Different predicted SL structures are numbered with roman numerals. Note that the lamin A 5'SS is in a single-stranded conformation, whereas the Progerin 5'SS is engaged in a secondary structure (referred to in the text as progerin SL). (B) The progeria mutation opens RNA structure around the progerin 5'SS. Autoradiographs show primer extension analyses of the WT progerin 5'SS and the mutant c.1824C>U progerin 5'SS cleaved by increased amount of T1 and T2 RNases. Lanes U, G, C and A correspond to the sequencing ladder. The dotted line at the level of the terminal G-C pair indicates that the stability of this terminal pair may be slightly decreased in the presence of the progeria mutation based on the appearance of some T2 RNase cleavage 3' to residue C1828.



proteins cross-linked to the progerin probes might be the SR proteins SRSF6 and one of the SRp30 proteins. Since the labeling of the 30 kDa band was decreased with the mutated RNA probe, it might represent SRSF1, which binding to the mutated progerin SL also decreased (Supplementary Material, Fig. S3). However, binding to other SRp30 proteins migrating at the same position of the gel (notably SRSF2 or SRSF7) cannot be completely rule out.

This identification was further confirmed by UV-cross-linking experiments performed with extracts from cells expressing tagged SRSF1 (His-SRSF1) or SRSF6 (Flag-SRSF6). Both tagged proteins were efficiently cross-linked, consistent with their expected apparent mobility (Fig. 3B, lanes 2, 3, 5 and 6) and were immunoprecipitated with the corresponding anti-tag antibodies (data not shown). Another confirmation was obtained by analyzing the cross-linked products with the WT RNA probe by two-D gel electrophoresis followed by western blotting. The 55 and 30 kDa cross-link signals coincided with different phosphorylation isoforms revealed by specific antibodies directed against SRSF6 and SRSF1, respectively (Fig. 3D, compare upper panel with SRSF1 and SRSF6 panels, respectively). To further document the specificity of the cross-linking, we tested two control probes under the same conditions: the RSF1 BS probe, which is a high-affinity binding site for RSF1 (RNA splicing repressor 1) known to bind hnRNP sequences (39), and the SRSF1 probe which is a high-affinity binding site for SRSF1 and other SR proteins (39). None of the probes demonstrated a strong signal at 55 kDa similar to the progerin SL probe (data not shown).

All the data of Figure 3 establish that the progerin SL and ESL RNAs have the ability to bind to SRSF1 and SRSF6. In these experiments, when protein SRSF1 was over-expressed, no significant decrease in the SRSF1 cross-link was detected in the presence of the mutation (Fig. 3B). However, in the presence of a more limited amount of SRSF1 (Fig. 3C and Supplementary Material, Fig. S3), the mutation was found to limit binding of SRSF1 to the RNA.

The SR protein SRSF6 represses splicing to the progerin 5'SS *in vitro*

To assess the contribution of the SRSF1 and SRSF6 splicing factors to progerin production, we cloned the *LMNA*

genomic sequence from exons 11 through 12 with or without the HGPS mutation in a reporter construct that was suitable for both cell transfection and *in vitro* splicing assays (Fig. 4A). In the presence of the HGPS mutation, transient transfections of these constructs in HeLa cells gave rise to a 150 nucleotide deletion in the *LMNA* splicing product due to the predominant use of the progerin 5'SS, whereas only the lamin A 5'SS was selected when using the WT *LMNA* reporter (Fig. 4B). In contrast, when the same constructs were used in *in vitro* splicing experiments (Fig. 4C), both the WT and mutated *LMNA* substrates led to the production of mRNAs arising from the utilization of both lamin A and progerin 5'SSs, implying that the progerin 5'SS can be recognized in the extract as an authentic 5'SS, even in the absence of the HGPS mutation. However, splicing in RNAs transcribed from the mutated *LMNA* construct predominantly used the progerin 5'SS, whereas in RNA of the WT *LMNA* construct splicing mostly proceeded through the lamin A 5'SS (Fig. 4C, compare lanes 4–7 and lanes 11–14). Depletion of the U1 snRNP from the extract abolished usage of both progerin and lamin A 5'SSs and led to exon 11 skipping (data not shown), implying that both splice sites are equally dependent on U1 snRNP. This result also indicate that exon 12 of *LMNA* may assemble a cross exon complex able to subsequently bind the globin 5'SS to generate a B-like spliceosomal complex to perform splicing independently of U1 as has recently been suggested by Schneider *et al.* (40).

To test whether SRSF1 or SRSF6 might be involved in activation of the utilization of the progerin 5'SS, *in vitro* splicing assays were performed with HeLa cell nuclear extracts supplemented with recombinant SRSF1 or SRSF6 proteins (Fig. 4D). An expected effect of the addition of a SR protein is to increase the global splicing activity of the nuclear extract. However, SRSF6 addition strongly inhibited the use of the progerin 5'SS, whereas the selection of the lamin A 5'SS was activated (Fig. 4D, compare lane 2 with lanes 3–4). Addition of SRSF1 to the extract also resulted in less progerin and more lamin A mRNA production from the WT substrate. But this effect was milder than that observed with SRSF6 (Fig. 4D, lanes 9–10). Similar effects of both SR proteins were obtained with the mutated *LMNA* transcript (Fig. 4D, lanes 6–7 and 12–13, respectively). However, SRSF6 had a very strong inhibition activity on the use of the mutated progerin 5'SS in the mutated RNA, whereas

Figure 4. SRSF1 and SRSF6 play opposite roles in *LMNA* splicing. (A) Schematic representation of the minigene reporters β globin-*LMNA* used for the study of *LMNA* splicing. *LMNA* sequences, carrying (Mut) or not carrying (Wt) the mutation, were inserted downstream of sequences derived from the human β globin gene. (B) These minigenes were transfected into HeLa cells and the splicing products were analyzed by RT-PCR of RNA extracted from transfected cells using primers either side of the alternatively spliced regions that give different sized products for the long and short forms. (C) Time course of *in vitro* splicing of WT and Mut reporters showing differential but significant use of both lamin A 5'SS and progerin 5'SS in HeLa nuclear extracts. RNA size markers are indicated on the left. Different times of incubation in minutes are indicated on the top of each panel. (D) Splicing reactions with Wt (lanes 1–4 and 8–10) and Mut (lanes 5–7 and 11–13) reporters in HeLa nuclear extracts alone (lanes 2, 5, 8 and 11) or supplemented with either SRSF6 (lanes 3–4 and 6–7) or SRSF1 (lanes 9–10 and 12–13) recombinant proteins [200 ng (lanes 3, 6, 9 and 12) or 400 ng (lanes 4, 7, 10 and 13)]. (Star) Note that a minor mRNA species of 450 nt long which accumulates in the presence of SRSF6 corresponds to the use of a cryptic 5'SS. (E) Splicing reactions with WT (lanes 1–6) and Mut (lanes 7–11) reporters mutated at lamin 5'SS in HeLa nuclear extracts alone (lanes 2 and 7, respectively) or supplemented with either SRSF6 (lanes 5–6 and 10–11) or SRSF1 (lanes 3–4 and 7–8) recombinant proteins [200 ng (lanes 3, 5, 8 and 10) or 400 ng (lanes 4, 6, 9 and 11)]. The relative efficiency of splicing is indicated below each panel, with a value of 100 for the assays without added SR protein. (F) Depletion of SRSF1 or SRSF6 in HeLa cells using siRNAs was assessed by western blotting and (G) resulting mRNA levels assessed by RT-qPCR. (H) The splicing pattern of the mutant β globin-*LMNA* reporter in treated cells was determined by RT-PCR using primers either side of the alternative spliced region as in (B) and (I) quantification of the ratio between truncated and full-length isoforms from three independent experiments of SRSF1 and SRSF6 siRNA knockdown. The value of 1 is arbitrarily assigned to control siRNA samples.

SRSF1 was unable to inhibit it completely. Also, SRSF6 highly activated the use of the lamin A 5'SS (Fig. 4D, lanes 6–7).

As these experiments could not discern whether SRSF6 acts as a repressor of the progerin 5'SS and/or as an activator of the lamin A 5'SS, we mutated the first G of the lamin A 5'SS in the WT and mutated substrates and tested the effect of SRSF6. Addition of SRSF6 to the extract inhibited strongly progerin mRNA production in the WT and the mutant context (Fig. 4E, compare lanes 2 and 7 with lanes 5–6 and lanes 10–11, respectively). In contrast, addition of SRSF1 had a mild effect in the WT context, and almost no effect in the presence of the c.1824C>T mutation (Fig. 4E, compare lanes 2 and 7 with lanes 3–4 and lanes 8–9, respectively), which is in agreement with its lower association with the mutated progerin SL RNA in HeLa nuclear extract. Taken together, the data suggest that the SRSF1 activity mainly consists in the activation of the lamin A 5'SS, while SRSF6 acts as a repressor of progerin production, most probably by binding to the progerin SL sequence and may be also by an independent activation of the lamin A 5'SS.

The SR protein SRSF6 represses the usage of the progerin 5'SS in transfected cells

If SRSF6 plays an important role in repressing the progerin 5'SS *in vivo*, it should be possible to reverse this phenomenon by decreasing SRSF6 levels. This possibility was next investigated by using small-interfering RNAs (siRNAs) to reduce the amount of SRSF6 in HeLa cells transfected with the mutant *LMNA* minigene, for which the selection of the progerin 5'SS is predominant. Treatment of HeLa cells with siRNAs targeting SRSF6 resulted in a large and specific reduction in the SRSF6 level, as observed 96 h post-transfection by western blotting (Fig. 4F). Under the same conditions, no significant changes were observed in the expression of SRSF1 and γ -tubulin, used as internal controls (Fig. 4F). Quantitative polymerase chain reaction (PCR) analysis also confirmed that SRSF6 expression was reduced at the RNA level (Fig. 4G). The effect of SRSF6 depletion on the splicing profile of the HGPS mutant *LMNA* minigene was analyzed by reverse transcription polymerase chain reaction (RT-PCR), using primers allowing discrimination between mRNAs spliced at the lamin A and the progerin 5'SSs, respectively (Fig. 4H). Results from three independent experiments showed that the siRNA-mediated reduction in the SRSF6 protein level greatly enhanced usage of the progerin 5'SS (Fig. 4H and I), whereas utilization of the lamin A 5'SS remained unchanged.

Surprisingly, siRNA knockdown of SRSF1 to comparable levels of SRSF6 knockdown (Fig. 4F and G) leads to the opposite effect on *LMNA* splicing, as it reduces usage of the progerin 5'SS (Fig. 4H and I). Since SRSF1 has only a limited affinity for the progerin SL, and since it did not activate the progerin 5'SS *in vitro*, the effect observed upon siRNA knockdown of SRSF1 might result from an indirect mechanism. Given that *in vivo* transcription and splicing are coupled (41), it is possible that SRSF1 depletion alters the transcription rate of the RNA pol II (42) allowing better recognition of the progerin 5'SS.

The SR proteins SRSF6 and SRSF1 have opposing effect on the usage of the progerin 5'SS in primary patients' fibroblasts

To directly demonstrate the involvement of SRSF1 and SRSF6 in the regulation of the progerin 5'SS selection, we used fibroblasts isolated from HGPS patients. The levels of SRSF1 or SRSF6 in these fibroblasts were reduced by RNAi-mediated knockdown and the splicing profile of endogenous *LMNA* was evaluated by RT-PCR using primers located in exon 8 and exon 12 to amplify both progerin and lamin A cDNAs. Consistent with the results obtained with transfected reporter constructs, the siRNA-mediated reduction in SRSF6 (Fig. 5B, panel SRSF6) greatly enhanced usage of the progerin 5'SS (Fig. 5A) with concomitant reduction in the lamin A 5'SS utilization. In contrast, SRSF1 knockdown (Fig. 5B, panel SRSF1) allowed slightly more lamin A mRNA production, whereas progerin mRNA levels remained unchanged (Fig. 5A). HGPS fibroblasts treated with siRNA targeting SRSF6 accumulated slightly more progerin than HGPS fibroblasts treated with control siRNA, as judged by western blotting with a lamin A/C antibody (Fig. 5B, panel lamin A/C). However, in keeping with the RNA analysis, the effect of SRSF1 knockdown on progerin expression is less visible. Taken together, these observations established conclusively that SRSF6 is directly responsible for repression of the progerin 5'SS in cells, in agreement with the effects of SRSF6 observed in *in vitro* splicing assays.

The progerin 5'SS splicing mechanism is conserved in the mouse

The mouse *LMNA* gene has 83% identity in the open reading frame when compared with human. Furthermore, the 20 nt long sequences surrounding the progerin 5'SS in the mouse (position 1817–1837) and human (position 1814–1834) mRNAs only show one nucleotide difference (U 1831 in the mouse instead of a C 1828 in human). Therefore, sequestration of the putative progerin 5'SS in a secondary structure in the mouse similar to that in human could be predicted (Fig. 6A), and we verified this hypothesis experimentally (Fig. 6B). We also showed that introduction of the human HGPS mutation at the same position in the mouse as in the human progerin SL (c.1827 C>U) strongly increased the accessibility of the terminal loop as found for the human pre-mRNA, implying that this conserved structure likely has a functional importance (Fig. 6B) and that the progerin 5'SS could be used in mice.

To determine whether regulation of the progerin 5'SS was similar in the two species, the HGPS C>T mutation was introduced 6 nt downstream from the progerin 5'SS (c.1827 C>T) in the *Lmna* mouse gene and mutated mice were generated by homologous recombination (Osorio *et al.*, submitted for publication). To evaluate the splicing profile of endogenous *LMNA* transcripts, RNA extracted from different mouse tissues of WT homozygous and heterozygous knock-in mice were submitted to RT-PCR using primers located in exon 8 and exon 12 to amplify both progerin and lamin A cDNAs (Supplementary Material, Fig. S4a). This analysis was performed with 4-month-old mice because all the homozygous knock-in mice *Lmna*^{G609/G609} died at this age (Osorio *et al.*, submitted

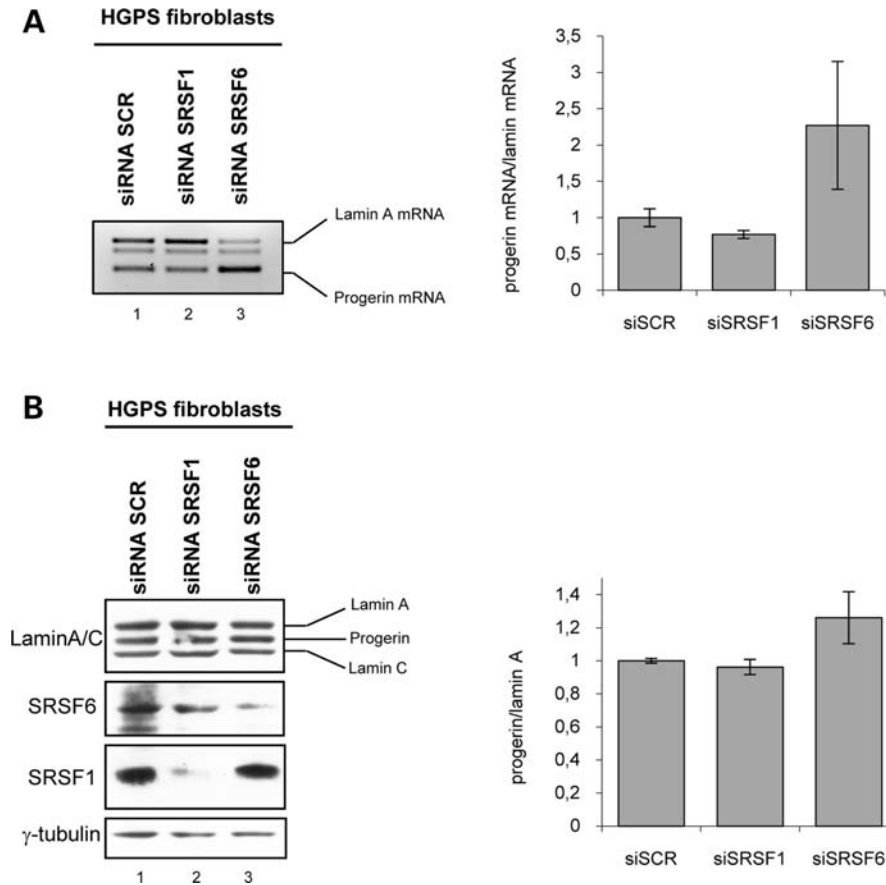


Figure 5. SRSF6 prevents usage of progerin 5'SS in fibroblasts from progeria patients. (A) The levels of lamin A/C and progerin mRNA in treated cells with scrambled siRNAs (lane 1) and with siRNA targeting either SRSF1 (lane 2) or SRSF6 (lane 3) were determined by RT-PCR using primers located in exon 9 and exon 12. Right panel quantification of the ratio between truncated and full-length isoforms from two independent experiments of SRSF1 and SRSF6 siRNA knockdown. (B) Depletions of SRSF1 or SRSF6 in fibroblasts from progeria patients using siRNAs (panels SRSF1 and SRSF6, respectively), and their effects on lamin A, lamin C and progerin expression (panel Lamin A/C), as assessed by western blotting. Right panel quantification of the ratio between progerin and lamin A from two independent experiments of SRSF1 and SRSF6 siRNA knockdown. The value of 1 is arbitrarily assigned to control siRNA samples.

for publication). As expected, both heterozygous and homozygous knock-in but not WT mice expressed progerin mRNA in all tissues (Supplementary Material, Fig. S4a). Both RT-PCR and western blot analysis of extracts from various tissues of 4-month-old homozygous knock-in mice (*Lmna*^{G609G/G609G}) confirmed that the steady-state levels of progerin are very high compared with the lamin A level which is hardly detectable in most tissues (Supplementary Material, Fig. S4a and b, G609G/G609G), implying that the expression of progerin from the mutant allele is predominant over lamin A in most tissues. Consistently, in heterozygous mice where both alleles are expressed, the levels of lamin A and progerin are comparable (Supplementary Material, Fig. S4a and b, G609G/+), whereas in WT mice only lamin A is expressed (Supplementary Material, Fig. S4a and b, +/+). *Lmna*^{G609G/G609G} mice also showed markedly reduced survival compared with WT littermates, since all the homozygous mice died 4 months after birth (Osorio *et al.*, submitted for publication). Strikingly, *Lmna*^{G609G/+} mice were also short lived but survived longer than homozygous mice (8 months on average) (Osorio *et al.*, submitted for publication), suggesting that *Lmna* splicing that favors progerin production can lead to reduced growth and lifespan.

In order to study the contribution of SR protein to the regulation of progerin production, we generated MEFs. MEFs isolated from WT, heterozygous (*Lmna*^{G609G/+}) and homozygous (*Lmna*^{G609G/G609G}) c.1827 C>T mutant embryos at embryonic day 13.5 were harvested to analyze the RNA splicing ratio and protein levels using RT-PCR and western blots, respectively (Fig. 6C and D). As expected, both heterozygous and homozygous but not WT MEFs expressed progerin mRNA (Fig. 6C) and protein (Fig. 6D), demonstrating that the c.1827 C>T mutation, like in human fibroblasts from progeria patients, activates the progerin 5'SS. In keeping with the PCR results, more progerin is produced in the homozygous compared with the heterozygous MEFs (Fig. 6D). However, while the c.1827 C>T mutation induces a large decrease in the expression of the lamin A, it did not abolish its expression in the homozygous MEFs, implying that alternative splicing is controlling the balance between lamin A and progerin expression. Consistent with previous results, immunofluorescence microscopy revealed that heterozygous and homozygous MEFs had more misshapen nuclei with nuclear blebs than WT MEFs (Fig. 6E and F). Thus, the c.1827 C>T mutation of the mouse *Lmna* gene reproduces the splicing-dependent phenotype of fibroblasts from progeria patients.

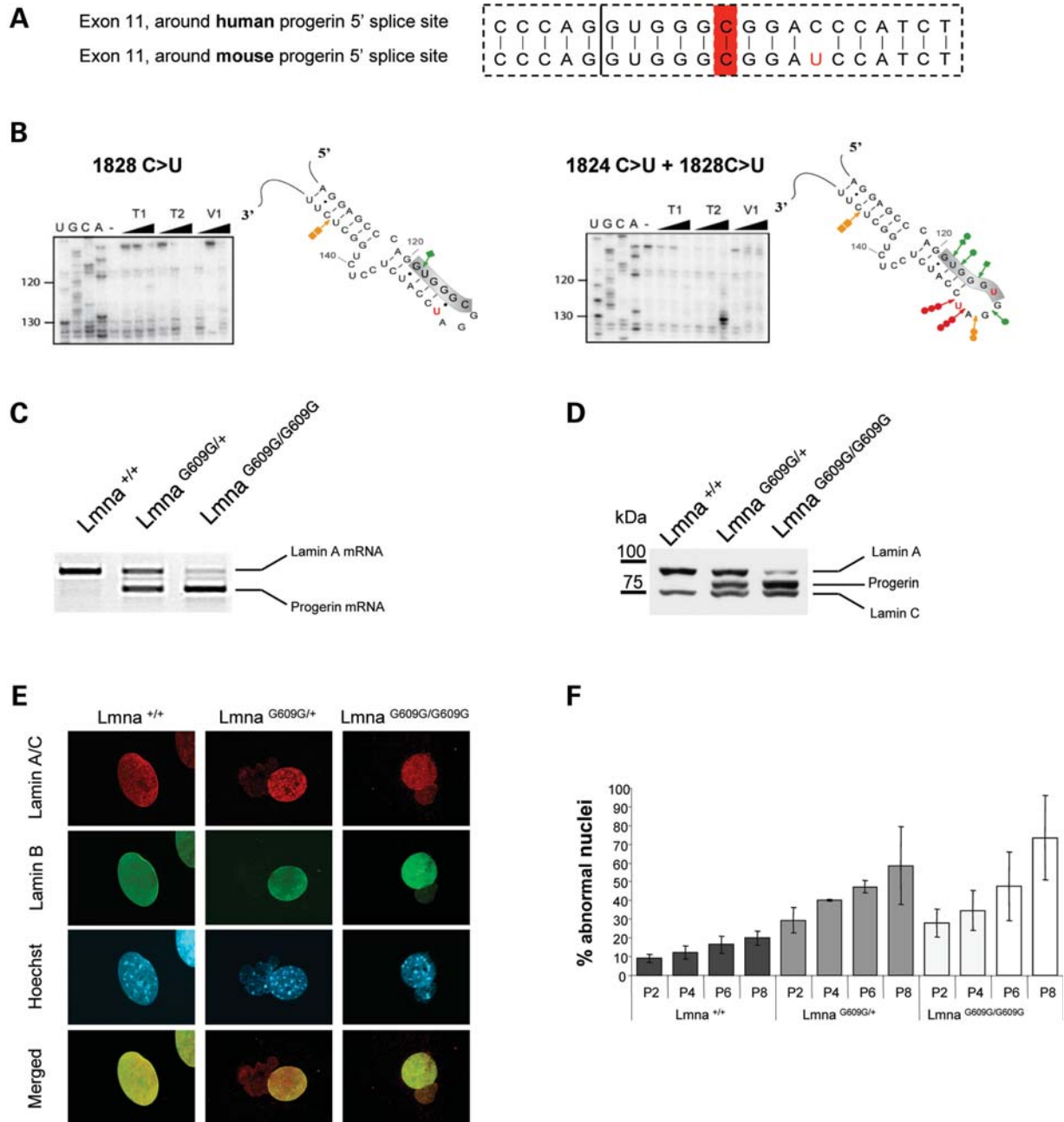


Figure 6. The use of progerin 5'SS is conserved from the mouse to human. (A) Sequence comparison between the mouse (position 1817–1837) and human (position 1814–1834) mRNAs corresponding to the progerin SL. (B) The secondary structure model proposed for WT (left) and mutated (right) mouse progerin SL. The model was proposed based on thermodynamic considerations and on the results of the enzymatic digestions shown. T1, T2 and V1 RNase cleavages are symbolized as in Figure 2. The structure representation shows all the bases used and the position of the progerin 5'SS is indicated. Autoradiographs show primer extension analyses of the WT and the mutant c.1827C>U mouse progerin SL cleaved by increasing amounts of T1, T2 and V1 RNases. Lanes U, G, C and A correspond to the sequencing ladder. Note good accessibility to T1 and T2 cleavage around the mutation. (C) Heterozygous (*Lmna*^{G609G/+}) and homozygous (*Lmna*^{G609G/G609G}) MEFs carrying the equivalent splicing mutation in endogenous *LMNA* express increased amounts of progerin as shown at the RNA level by RT-PCR using primers either side of the mutation and (D) at the protein level as shown by western blotting revealed with lamin A/C antibody. (E) Expression of mouse progerin leads to nuclear abnormalities, as shown by immunofluorescence with anti-lamin A/C and Hoechst staining. Scale bars correspond to 10 μ m. (F) Quantification of nuclear abnormalities in WT (*Lmna*^{+/+}), *Lmna*^{G609G/+} and *Lmna*^{G609G/G609G} mutated fibroblasts at the indicated cell passages.

Next, to test whether SRSF1 and/or SRSF6 modulate the progerin 5'SS *in vivo*, we reduced their levels with specific siRNAs in *Lmna*^{G609G/+} MEFs. *Lmna*^{G609G/+} MEFs were either mock-treated or transfected with siRNAs directed against SRSF1 or SRSF6 and the corresponding proteins

levels were assessed by western blot analysis 5 days after transfection. A reduction in both protein levels was observed with their corresponding siRNAs (Fig. 7A, upper and lower panels). To test the effect of SR protein depletion on the splicing profile of *LMNA* primary transcripts expressed in the

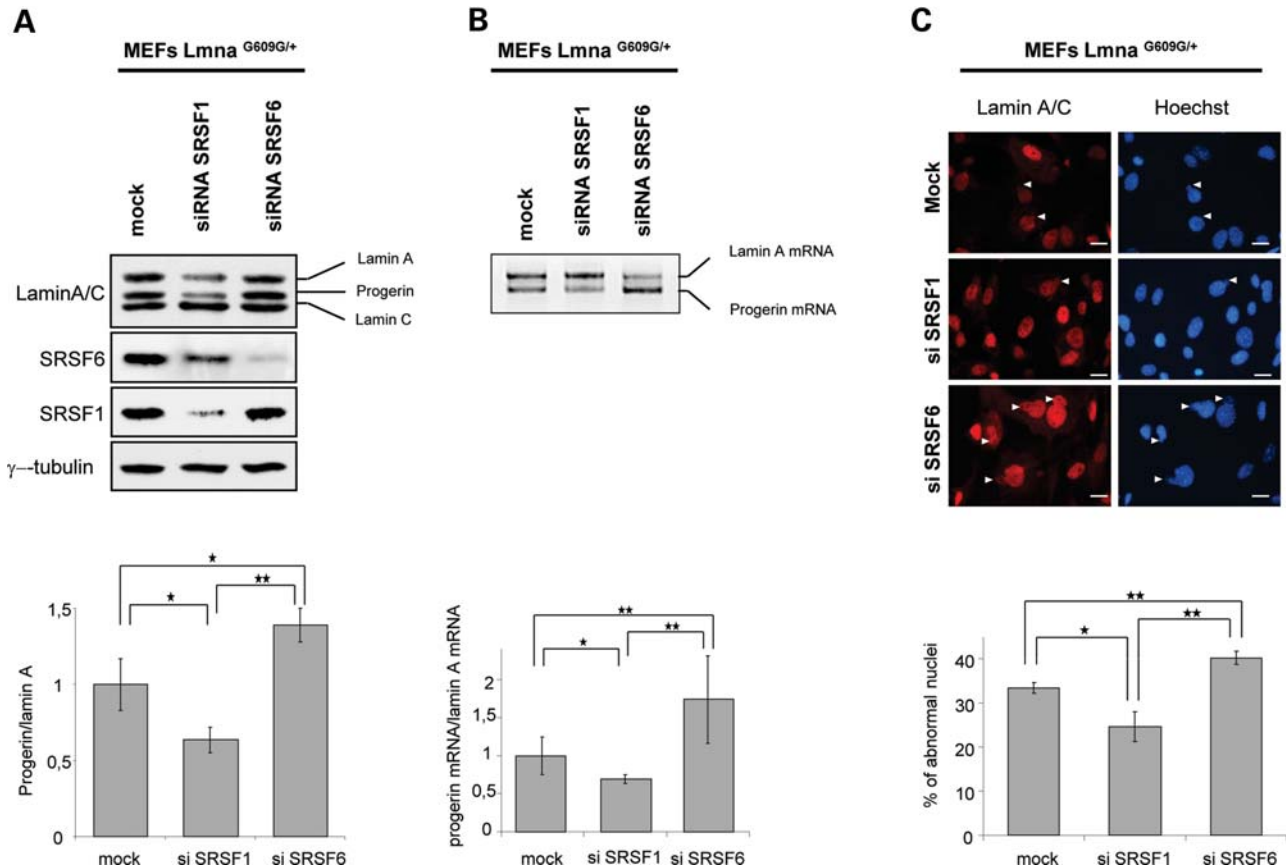


Figure 7. *LMNA* splicing regulation by the SR proteins SRSF1 and SRSF6 is conserved between the mouse and human. SRSF1 or SRSF6 was depleted in *Lmna*^{G609G/+}MEFs using siRNAs. Below each section, the quantifications are shown as bar charts. (A) Western blot showing depletion of SRSF1 or SRSF6 and its effect on the ratio of lamin A/C and progerin. (B) The splicing pattern of the *LMNA* gene in SRSF1 or SRSF6 depleted cells was determined by RT-PCR and analysed as in Figure 5C. (C) Nuclear abnormalities in *Lmna*^{G609G/+} MEFs after SRSF1 or SRSF6 depletion, as shown by immunofluorescence with anti-lamin A/C and Hoechst staining. Scale bars correspond to 30 μ m. Percentage of nuclear abnormalities in siRNA-treated versus control cells is shown.

corresponding fibroblasts, RT-PCR experiments were performed with an oligonucleotide pair allowing amplification of both lamin A and progerin isoforms. The results established that siRNA-mediated reduction in SRSF6 protein levels is correlated to an effective increase in progerin both at the protein (Fig. 7A, upper and lower panels) and mRNA levels (Fig. 7B, upper and lower panels), whereas siRNA-mediated reduction in SRSF1 leads to opposite effect (Fig. 7A and B, upper and lower panels). Given that progerin accumulation was expected to change the nuclear envelope of MEFs, we checked the effect of these SR proteins depletion on nuclear morphology. As predicted, depletion of SRSF6 was associated with more misshapen nuclei, whereas SRSF1 depletion reduced the number of misshapen nuclei. Taken together, these observations establish for the first time that SRSF6 and SRSF1 have opposing effect on *Lmna* gene splicing.

DISCUSSION

In 2003, it was discovered that the silent mutation in exon 11 of the *LMNA* gene responsible for human progeria syndrome allows production of progerin by inducing utilization of a 5'SS in the exon 11 (4,5). Although this phenomenon was

described long ago, the molecular basis for the age-associated splicing alteration of the *LMNA* gene has not been elucidated. Here we demonstrate that the 5'SS in the exon 11 of the *LMNA* gene is engaged in a stable RNA structure which is probably preventing its efficient recognition by the splicing machinery. The progeria mutation induces some opening of the terminal loop which may favor accessibility of the internal 5'SS and facilitate U1 snRNP association. In addition, regulation of the competition between the progerin 5'SS and lamin A 5'SS by the SR proteins SRSF1 and SRSF6 is also modulated by the mutation. The demonstration that these two characteristic features are also conserved in the mouse further underlies the importance of splicing repression to minimize progerin production during aging.

It is indeed striking that the progerin 5'SS is conserved in mammals over millions of years and that the single-point mutation at the normally uninfluential +6 position leads to the same dramatic changes in splicing. Our *in vitro* splicing analyses of the WT and mutated *LMNA* pre-mRNA, performed for the first time, showed that WT progerin 5'SS is a *bona fide* 5'SS, since it is moderately recognized from the WT transcript, and strongly activated from the mutated transcripts, as expected (Fig. 4). Interestingly, our observation of the utilization of the WT progerin 5'SS in the absence of the mutation

is in agreement with several reports indicating that progerin may be detected at low level during physiological aging (10,15–17). Furthermore, the fact that the splicing at the progerin 5'SS can be also induced in WT fibroblasts using anti-sense oligonucleotides against exon 11 sequences (43), and that the splicing of WT and mutated *LMNA* transcripts is modulated by SR proteins strongly supports the idea that the progerin 5'SS is an alternative 5'SS. Therefore, the mutation 1824C>T reinforces a naturally weak 5'SS rather than create a *de novo* 5'SS.

Interestingly, the progerin 5'SS in the WT exon 11 is engaged in a stable SL structure (progerin SL), with a compact terminal tetra-loop. This tight structuration likely prevents its efficient recognition by the splicing machinery. In contrast, the lamin A 5'SS is in a favorable non-structured region (Fig. 2). The progeria mutation markedly increases the accessibility of the terminal loop of the progerin SL, which together with the slight increase in the intrinsic strength of the progerin 5'SS by the C>U substitution is expected to favor the recognition of the 5'SS by U1 snRNP. Indeed, it is well known that RNA–RNA interaction preferentially initiates through loop–loop or single strand–loop interactions (44). Interestingly, we observed that the other mutation 1822 G>A in the human *LMNA* gene, which is associated with HGPS (4,5), also leads both to an opening of the progerin SL structure and an increased progerin 5'SS utilization. It will be interesting to identify the kind of structuration of the progerin SL terminal loop by structural analysis such as NMR 3D structure analysis, since another single mutation in this loop, 1825 G>A, was found to induce both an opening of the loop structure and an increase in the progerin 5'SS utilization *in vitro*. We predict that the occurrence of this mutation in the human *LMNA* gene may generate HGPS. In support to the proposed role of the RNA structure in regulation of the progerin 5'SS, it should be pointed out that there are already well-documented examples for the involvement of RNA secondary structure in the control of alternative splicing (31,45,46). For example, the stability of a predicted SL structure at the 5'SS of the key Alzheimer's protein tau regulates usage of exon 10 (47,48) and the alternative exon of the key adhesion gene fibronectin is highly influenced by secondary RNA structure (31). Bioinformatics analyses indicate that the splicing regulatory sequences are preferentially in a single-stranded conformation, as this allows these sequences to interact with RNA-binding proteins that mostly have a preference for single-strand RNA (45). At present, it is unclear whether SR proteins SRSF6 and SRSF1 that regulate the progerin 5'SS utilization are involved in the stabilization or disruption of the identified RNA structure. According to the present data, SRSF6 might stabilize the RNA structure around the progerin 5'SS, thereby, preventing SRSF1 from enhancing the recruitment of the U1 snRNP. As transcription and splicing are connected, the kinetics of elongating polymerase could also influence the formation of RNA structures in connection with SR protein concentrations (26,41).

Like other splicing mutations that are involved in the etiology of human diseases, the HGPS mutation does not inactivate *LMNA* gene expression completely, but rather gives rise to a mixture of normal and aberrant isoforms. Transitions between splicing isoforms are dynamic and depend on a

balance between factors that maintain a silent alternative splice site and those that promote its activation, possibly in a tissue-specific manner (19). Increased production of progerin in the homozygous and heterozygous mice harboring the splicing mutation triggers many of the features that appear early on in humans with HGPS, such as slow growth, osteolytic lesions in bone, osteoporosis, micrognathia and loss of adipose tissue (Osorio *et al.*, submitted for publication). In contrast, consistent with previous reports (49) (Osorio *et al.*, submitted for publication), no functional abnormalities were associated with mice lacking lamin A and/or progerin expression, indicating that progerin, even at trace levels, could be detrimental for lifespan. Given that progerin production is under the control of both transcription and splicing of the *LMNA* gene, the importance of splicing has escaped analysis in previously described models (50,51). If changes in the RNA structure and/or SR proteins concentrations occur preferentially in some tissues but not others, one would expect that progerin accumulation will also be different between tissues. Our initial analysis of progerin expression in various tissues of the mouse shows that this is indeed the case (Supplementary Material, Fig. S4). In WT mice, where only lamin C and lamin A are detected, it can be clearly seen that while the brain contains roughly equivalent amount of both proteins, in all other tissues the lamin A content is higher than lamin C. Also, the brain accumulated less progerin than lamin C in both homozygous and heterozygous knock-in mice. Consistent with the RNA analysis, in heterozygous knock-in mice, it can be appreciated that less progerin is expressed in both the brain and spleen where the lamin A mRNA was higher than progerin mRNA. In contrast, the heart of heterozygous mice accumulated more progerin than any other tissue.

The detailed knowledge of the factors that are critical for the activation described here and how they cooperate with other spliceosomal components in a given tissue in the HGPS-like mouse model will help the design of new therapeutic agents. The basis for targeting mutated RNA sequences is straightforward and highly specific for a given gene because it relies on antisense molecules base-paired to pre-mRNA to prevent access of the splicing machinery to splice sites (52,53). Combination of the RNA structure and binding of SR proteins described here helps explain past successes and failures of anti-sense oligonucleotides (ASOs) to modulate alternative splicing within *LMNA* exon 11 (43,53). Conversely, we show here that the region 50 nucleotides downstream of the alternative donor site is fully accessible and may serve as binding site for splicing regulators. Interestingly, targeting of ASOs to that region was effective at triggering progerin production from WT *LMNA* pre-mRNA (43,53). It has been postulated that this enhancement might be due to the ability of ASOs to hide a binding site for SRSF5. Our *in vitro* complementation assay is in keeping with this postulate because SRSF5 is shown to enhance the use of the *LMNA* 5'SS at the expenses of progerin 5'SS (43) (data not shown). Our finding that two SR proteins might have opposing effects on progerin 5'SS utilization indicates that the efficiency of ASOs to prevent splicing at this site will depend on the cellular concentration of the two SR proteins, making the outcome of the effect of the ASOs less predictable. This does indeed seem to be the case since in one study a morpholino ASO

hybridizing to the progerin 5'SS was shown to be effective at reducing the aberrant splicing, whereas another study using a 2'O methyl ASO had a negligible effect (43,54).

The new mouse model (Osorio *et al.*, submitted for publication) will facilitate testing the outcomes of ASO treatment in different tissues; it could also lead to development of a therapeutic strategy involving small molecules that target splicing factors (53,55). This can be achieved either by lowering their cellular levels or by interfering with their splicing enhancing/repressing activity. Our data establish a proof of principle that SR proteins could be therapeutic targets. RNAi-mediated reduction in the SR protein SRSF1 levels led to a reduction in progerin expression in heterozygous *Lmna*^{G609G/+} MEFs, whereas SRSF6 knockdown aggravated the MEFs phenotype. As SR protein knockdown is expected to have a pleiotropic effect on gene expression and not only affect progerin expression, targeting of the activity of SR proteins on specific substrates could be more attractive. Indeed, screening of chemical libraries with ESE-dependent splicing substrates resulted in the identification of indole derivatives as a class of small molecule inhibitors of alternative splicing (56). Rather than generally inhibiting splicing, these molecules proved highly selective for splicing events mediated by different classes of ESE sequences and are therefore less toxic. Their selectivity is thought to depend on their interaction with each SR protein (56,57). Further studies are now ongoing to confirm the potency and lack of deleterious side-effects of indole derivatives in the HGPS model.

The control of lamin A/progerin splicing switch of the *LMNA* gene in the various tissues of the mouse will have an important impact on the lifespan. Balancing this output in critical tissues will be a major determinant not only for therapeutic action but also for establishing the longevity of mammalian organisms.

MATERIALS AND METHODS

Ethics statement

All animal procedures were conducted in strict adherence with the European Community Council Directive of 24 November 1986 (86-609/EEC).

Plasmids constructs

LMNA sequences (exon 11, intron 11 and exon 12) were PCR amplified from WT and patient's cell genomic DNA with specific forward and reverse primers. PCR fragments were purified with Concert Rapid PCR purification system (Invitrogen) and subcloned at the *Bam*HI and *Eco*RI restriction sites of the β glo3S plasmid (39) to give the β Glo-*LMNA* constructs used for *in vitro* splicing and transient transfection experiments.

Cell lines, culture and transfection conditions

HeLa cells were grown in Dulbecco's modified eagle medium media (Gibco) complemented with 10% fetal calf serum and antibiotics. They were transfected in six-well plates, at 50% confluency (30% for siRNA experiments), using Dreamfect

(OZ biosciences) for plasmid DNA or oligofectamine (Invitrogen) for siRNAs, according to the manufacturer's instructions. For siRNA depletion of SR proteins, cells were treated for 72 h with siRNAs against hASF/SF2 (hSRSF1) or 96 h with siRNAs against hSRSF6 (with two successive applications carried out at 24 h interval). The mutant β Glo-*LMNA* plasmid was transfected and incubated for 24 h before recovering the cells. The siRNA sequences are available upon request. MEFs were derived from embryos dissected 13.5 days after detection of vaginal plugs according to Nagy *et al.* (58). Fetal livers and/or yolk sacs were used for PCR genotyping. MEFs were transfected in six-well plates with siRNA using oligofectamine (Invitrogen), according to the manufacturer's instructions. For siRNA depletion of SR proteins, cells were treated for 72 h with siRNAs against mSRSF1 or 96 h with siRNAs against mSRSF6 (with two successive applications carried out at 24 h interval). The siRNA sequences are available upon request.

Human HGPS fibroblasts AG01972 were purchased from Coriell Cell Repository. They were cultured at 37°C in DMEM containing GlutaMAX, non-essential amino acids, sodium pyruvate, 0.1 mM β -mercaptoethanol and 10% fetal bovine serum. For siRNA depletion of SR proteins, cells were treated for 72 h with siRNAs against SRSF1 or SRSF6. The siRNA sequences are available upon request.

Expression of tagged SR proteins SRSF6-Flag and SRSF1-His was performed after transfection of the corresponding plasmid in the human embryonic kidney 293 cell line expressing Epstein-Barr virus EBNA1 protein (293E) according to the established protocol (59).

RNA and protein analysis

RNAs were extracted using TRI Reagent (Sigma-Aldrich). The samples were treated with RNase-free DNase (RQ1, Promega). Cellular RNA concentrations were quantified by measuring optical absorption at 260 nm with a nanodrop. 1.5 μ g of RNA was reversed transcribed using 'First strand cDNA synthesis' kit (GE Healthcare biosciences) with random hexamers. PCRs were carried out with 0.1 mM dNTP mix, 1 mM MgCl₂, 1 \times PCR buffer, 1.25 U of Taq DNA polymerase (Invitrogen) and 0.2 μ M of each of the sense and antisense primers. Denaturation, annealing and extension were performed at 94, 64 and 72°C, respectively. Each step lasted 30 s. PCRs were performed on a Master cycler Gradient 96 thermocycler (Eppendorf) with 28 cycles. These cycles were preceded by a 3 min denaturation at 94°C and terminated by a 2 min extension at 72°C. Amplification products were analyzed by 2% agarose gel electrophoresis and visualized by ethidium bromide staining. The intensity of the bands corresponding to the two mRNAs was quantified using GeneSnap acquisition software and GeneTools analysis software (Syngene). The ratio lamin A 5'SS/progerin 5'SS from three independent transfection experiments was normalized using the control sample of each series as a reference, which gave a score for the choice of progerin 5'SS.

HeLa cell proteins were extracted in a buffer containing 50 mM Tris-HCl pH 6.8, 20 mM ethylenediaminetetraacetic acid (EDTA), 5% sodium dodecyl sulfate (SDS), sonicated briefly on ice and analysed by SDS-PAGE and western

blotting. Proteins from MEFs and mouse tissues were extracted in a buffer containing 63 mM Tris-HCl pH 7.5, 2% SDS, 5% β -mercaptoethanol and 8 M urea. Samples were ground in a glass tissue grinder for additional 2 min and then sonicated and centrifuged at 13 200g for 10 min at 4°C. The supernatant was analyzed by western blotting using 4–12% polyacrylamide BisTris gels (Invitrogen) for electrophoresis and fractionated proteins were then transferred to a nitrocellulose membrane. For western blotting, we used the following antibodies with the corresponding dilutions: anti γ -tubuline (sigma) (1/1000); anti-ASF/SF2 (Invitrogen/Zymed, catalog #32-4500); anti-SRSF6 (kind gift of Adrian Krainer) (mAb 8-1-28 culture supernatant); anti-lamin A/C (Santa Cruz, sc-20681); anti-mouse HRP (GE Healthcare) and anti-rabbit HRP (GE Healthcare).

Immunofluorescence

MEFs were plated on glass cover slips at a confluence of 50% before fixation in 3.7% formaldehyde in phosphate-buffered saline (PBS) followed by a 5 min permeabilization in 0.1% Triton X-100 in PBS. Cells were then incubated in PBS containing 3% bovine serum albumin (BSA) before staining with primary antibodies as follows: rabbit polyclonal anti-lamin A/C (N-18) (sc-6215 from Santa Cruz Biotechnology, Inc.) at 4 μ g/ml in PBS–0.1% BSA, goat polyclonal anti-lamin B (M-20) at 4 μ g/ml in PBS–0.1% BSA (sc-6217 from Santa Cruz Biotechnology, Inc.). Primary antibodies were revealed with either an AlexaFluor546- or -488-conjugated anti-rabbit or anti-goat antibody (Invitrogen). Nuclei were stained with Hoechst 33 342 dye (1 μ g/ml) (Sigma B2261). Cells were then washed in PBS and mounted on glass slides in 'ProLong Gold Antifade' Reagent (Invitrogen). Sixteen-bit fluorescent images were captured with a MetaMorph-driven microscope (Leica DM6000) using a Leica 40 HCX PL APO 1.25-0.75 oil immersion objective (Leica) and a 'CoolSNAP HQ2' camera (Photometrics). Individual images were further processed using Adobe Photoshop software.

Recombinant proteins and *in vitro* and *ex vivo* splicing assays

Recombinant SRSF1 and SRSF6 were produced and purified from baculovirus-infected Sf9 cells as previously reported (60). For *in vitro* splicing, radiolabelled RNAs were synthesized by *in vitro* transcription in the presence of 50 U of T7 RNA polymerase (NEB), 2 μ g of the suitable linearized plasmids and 50 μ Ci [α -³²P] UTP (800 Ci/mmol) in 40 μ l reactions according to the manufacturer conditions. After DNase (RQ1, PROMEGA) digestion, *in vitro* transcripts were purified with sigma columns (Sigma, RTN10-1K) and quantified by Cerenkov counting. Splicing reactions with HeLa nuclear extracts (CilBiotech) and 20 fmol of radiolabelled transcripts were performed under standard conditions as described previously (61). Spliced products were cleaned by proteinase K-treatment and phenol extraction, and analyzed by 6% polyacrylamide gel electrophoresis.

UV cross-linking

For UV cross-linking, radiolabelled RNAs were synthesized by *in vitro* transcription in the presence of 20 U of SP6 RNA polymerase (NEB), 1 μ g of the suitable linearized plasmids and 60 μ Ci [α -³²P] GTP (800 Ci/mmol) in 20 μ l reactions according to the manufacturer's instructions. *In vitro* transcripts were purified by phenol-chloroform extraction, verified by denaturing polyacrylamide-urea gel electrophoresis and quantified by Cerenkov counting. HeLa nuclear extracts were pre-incubated for 15 min at 37°C in a 10 μ l solution containing 10 mM triethylamine (TEA) pH 8, 50 mM KCL, 0.1 mM EDTA, 0.25 mM DTT, 10% glycerol, 7.5 mM ATP, 25 mM creatine phosphate, 1 mM MgCl₂ and 0.025 μ g/ μ l of yeast tRNA. One hundred femtomole of indicated radiolabelled RNA was then added into 10 μ l of interaction buffer (10 mM TEA pH 8, 50 mM KCL, 0.1 mM EDTA, 2.25 mM DTT, 12.6% glycerol, 0.75 mM ATP, 25 mM creatine phosphate, 1 mM MgCl₂, 0.2% NP40, 32 U of RNasin (PROMEGA) and 0.06 μ g/ μ l of BSA). Mixture reactions were then incubated 15 min at 30°C, and subsequently transferred to 96-well plates. Samples were irradiated for 20 min on ice with UV light (254 nm) at a distance of 5 cm. After RNase treatment, 20 μ l of 5 \times SDS gel loading buffer was added in each sample and cross-linked proteins were separated by 12% SDS-PAGE. Gels were fixed (30 min in 50% methanol, 10% acetic acid, then 5 min in 7% methanol, 7% acetic acid, 1% glycerol), dried and revealed by autoradiography.

For two-dimensional gel analysis of SR proteins, UV cross-linked proteins were diluted in a buffer containing 7 M urea, 2 M thiourea, and 4% CHAPS, 4% IPG buffer and 10 mM DTT. Samples were subjected to two-dimensional analysis first with Immobiline Dry strips (pH 3-11 NL GE healthcare) using an Ettan IPGphor3 IEF system (GE healthcare life sciences) according to the manufacturer's instructions. After the second dimension electrophoresis, proteins were transferred onto nitrocellulose membranes. The membrane was first revealed by autoradiography and then SRSF1 and SRSF6 were detected with the above indicated antibodies, followed by ECL staining.

Enzymatic and chemical probing of RNA secondary structure

RNA 2-D structures in solution were probed as follows; 200 ng of transcripts dissolved at a 80 nM concentration in buffer D (20 mM Hepes-KOH, pH 7.9, 100 mM KCl, 0.2 mM EDTA pH 8.0, 0.5 mM DTT, 0.5 mM phenylmethylsulfonyl fluoride, 20% (vol/vol) glycerol) were renatured by 10 min heating at 65°C, followed by slow cooling at room temperature with the addition of 1 μ l of 62.5 mM MgCl₂ to a final concentration of 3.25 mM MgCl₂. After a 10 min pre-incubation at room temperature, RNase T1 (0.02 or 0.0375 U/ μ l) or T2 (0.025 or 0.0375 U/ μ l) was added under conditions conducive to cleavage of single-stranded segments. V1 RNase (2.5 \times 10⁻³ or 5 \times 10⁻³ U/ μ l) was used to cleave double-stranded and stacked residues. DMS [1 μ l of a 1/4 or 1/8 (V/V) DMS/EtOH solution] was employed to modify single-stranded A and C residues and CMCT was used (4 or 5 μ l of a 180 mg/ml solution) to modify single-stranded U and to a lesser extent

G residues. Reactions were stopped as previously described (23). Cleavage and modification positions were identified by primer extension (23). Stable secondary structures having the best fit with experimental data were identified with the Mfold software, version 8.1. Probing data were introduced as a constraint in the search.

SUPPLEMENTARY MATERIAL

Supplementary Material is available at *HMG* online.

ACKNOWLEDGEMENTS

We thank A. Krainer for the gifts of antibodies against SRSF6. Thanks to members of the Tazi laboratory for helpful discussions. Special thanks to J. Venables for critical reading of the manuscript.

Conflict of Interest statement. None declared.

FUNDING

I.C.L.-M. and V.V. were supported by a graduate fellowships from the Ministère Délégué à la Recherche et aux Technologies. M.T. was supported by a post-doctoral fellowship of the Association Française contre les Myopathies (AFM) and CNRS. This work was supported by grants from the Agence Nationale de la Recherche (ANR-05-BLAN-0261-01) and the European Alternative Splicing Network of Excellence (EURASNET, FP6 life sciences, genomics and biotechnology for health). Ministerio de Ciencia e Innovación-Spain, PCTI-FICYT Asturias, European Union (FP7 MicroEnviMet), and Fundación M. Botin.

REFERENCES

- Lin, F. and Worman, H.J. (1993) Structural organization of the human gene encoding nuclear lamin A and nuclear lamin C. *J. Biol. Chem.*, **268**, 16321–16326.
- Nakajima, N. and Abe, K. (1995) Genomic structure of the mouse A-type lamin gene locus encoding somatic and germ cell-specific lamins. *FEBS Lett.*, **365**, 108–114.
- Machiels, B.M., Zorenc, A.H., Endert, J.M., Kuijpers, H.J., van Eys, G.J., Ramaekers, F.C. and Broers, J.L. (1996) An alternative splicing product of the lamin A/C gene lacks exon 10. *J. Biol. Chem.*, **271**, 9249–9253.
- Eriksson, M., Brown, W.T., Gordon, L.B., Glynn, M.W., Singer, J., Scott, L., Erdos, M.R., Robbins, C.M., Moses, T.Y., Berglund, P. *et al.* (2003) Recurrent de novo point mutations in lamin A cause Hutchinson-Gilford progeria syndrome. *Nature*, **423**, 293–298.
- De Sandre-Giovannoli, A., Bernard, R., Cau, P., Navarro, C., Amiel, J., Boccaccio, I., Lyonnet, S., Stewart, C.L., Munnich, A., Le, M.M. and Levy, N. (2003) Lamin A truncation in Hutchinson-Gilford progeria. *Science*, **300**, 2055.
- Dechat, T., Pflieger, K., Sengupta, K., Shimi, T., Shumaker, D.K., Solimando, L. and Goldman, R.D. (2008) Nuclear lamins: major factors in the structural organization and function of the nucleus and chromatin. *Genes Dev.*, **22**, 832–853.
- Worman, H.J., Fong, L.G., Muchir, A. and Young, S.G. (2009) Laminopathies and the long strange trip from basic cell biology to therapy. *J. Clin. Invest.*, **119**, 1825–1836.
- Worman, H.J. and Bonne, G. (2007) “Laminopathies”: a wide spectrum of human diseases. *Exp. Cell Res.*, **313**, 2121–2133.
- Varela, I., Cadinanos, J., Pendas, A.M., Gutierrez-Fernandez, A., Folgueras, A.R., Sanchez, L.M., Zhou, Z., Rodriguez, F.J., Stewart, C.L., Vega, J.A. *et al.* (2005) Accelerated ageing in mice deficient in Zmpste24 protease is linked to p53 signalling activation. *Nature*, **437**, 564–568.
- Scaffidi, P. and Misteli, T. (2008) Lamin A-dependent misregulation of adult stem cells associated with accelerated ageing. *Nat. Cell Biol.*, **10**, 452–459.
- Shumaker, D.K., Dechat, T., Kohlmaier, A., Adam, S.A., Bozovsky, M.R., Erdos, M.R., Eriksson, M., Goldman, A.E., Khuon, S., Collins, F.S. *et al.* (2006) Mutant nuclear lamin A leads to progressive alterations of epigenetic control in premature aging. *Proc. Natl Acad. Sci. USA*, **103**, 8703–8708.
- Glynn, M.W. and Glover, T.W. (2005) Incomplete processing of mutant lamin A in Hutchinson-Gilford progeria leads to nuclear abnormalities, which are reversed by farnesyltransferase inhibition. *Hum. Mol. Genet.*, **14**, 2959–2969.
- Dechat, T., Shimi, T., Adam, S.A., Rusinol, A.E., Andres, D.A., Spielmann, H.P., Sinensky, M.S. and Goldman, R.D. (2007) Alterations in mitosis and cell cycle progression caused by a mutant lamin A known to accelerate human aging. *Proc. Natl Acad. Sci. USA*, **104**, 4955–4960.
- Cao, K., Capell, B.C., Erdos, M.R., Djabali, K. and Collins, F.S. (2007) A lamin A protein isoform overexpressed in Hutchinson-Gilford progeria syndrome interferes with mitosis in progeria and normal cells. *Proc. Natl Acad. Sci. USA*, **104**, 4949–4954.
- McClintock, D., Ratner, D., Lokuge, M., Owens, D.M., Gordon, L.B., Collins, F.S. and Djabali, K. (2007) The mutant form of lamin A that causes Hutchinson-Gilford progeria is a biomarker of cellular aging in human skin. *PLoS ONE*, **2**, e1269.
- Haithecock, E., Dayani, Y., Neufeld, E., Zahand, A.J., Feinstein, N., Mattout, A., Gruenbaum, Y. and Liu, J. (2005) Age-related changes of nuclear architecture in *Caenorhabditis elegans*. *Proc. Natl Acad. Sci. USA*, **102**, 16690–16695.
- Rodriguez, S., Coppede, F., Sagelius, H. and Eriksson, M. (2009) Increased expression of the Hutchinson-Gilford progeria syndrome truncated lamin A transcript during cell aging. *Eur. J. Hum. Genet.*, **17**, 928–937.
- Will, C.L. and Luhrmann, R. (2001) Spliceosomal UsnRNP biogenesis, structure and function. *Curr. Opin. Cell Biol.*, **13**, 290–301.
- Black, D.L. (2003) Mechanisms of alternative pre-messenger RNA splicing. *Annu. Rev. Biochem.*, **72**, 291–336.
- Soret, J. and Tazi, J. (2003) Phosphorylation-dependent control of the pre-mRNA splicing machinery. *Prog. Mol. Subcell Biol.*, **31**, 89–126.
- Bourgeois, C.F., Lejeune, F. and Stevenin, J. (2004) Broad specificity of SR (serine/arginine) proteins in the regulation of alternative splicing of pre-messenger RNA. *Prog. Nucleic Acid Res. Mol. Biol.*, **78**, 37–88.
- Lin, S. and Fu, X.D. (2007) SR proteins and related factors in alternative splicing. *Adv. Exp. Med. Biol.*, **623**, 107–122.
- Hallay, H., Locker, N., Ayadi, L., Ropers, D., Guittet, E. and Branlant, C. (2006) Biochemical and NMR study on the competition between proteins SC35, SRp40, and heterogeneous nuclear ribonucleoprotein A1 at the HIV-1 Tat exon 2 splicing site. *J. Biol. Chem.*, **281**, 37159–37174.
- Marchand, V., Mereau, A., Jacquenet, S., Thomas, D., Mouglin, A., Gattoni, R., Stevenin, J. and Branlant, C. (2002) A Janus splicing regulatory element modulates HIV-1 tat and rev mRNA production by coordination of hnRNP A1 cooperative binding. *J. Mol. Biol.*, **323**, 629–652.
- Tazi, J., Bakkour, N. and Stamm, S. (2009) Alternative splicing and disease. *Biochim. Biophys. Acta*, **1792**, 14–26.
- Pandit, S., Wang, D. and Fu, X.D. (2008) Functional integration of transcriptional and RNA processing machineries. *Curr. Opin. Cell Biol.*, **20**, 260–265.
- Buratti, E., Muro, A.F., Giombi, M., Gherbassi, D., Iaconcig, A. and Baralle, F.E. (2004) RNA folding affects the recruitment of SR proteins by mouse and human polypurinic enhancer elements in the fibronectin EDA exon. *Mol. Cell Biol.*, **24**, 1387–1400.
- Caceres, J.F. and Kornblihtt, A.R. (2002) Alternative splicing: multiple control mechanisms and involvement in human disease. *Trends Genet.*, **18**, 186–193.
- Ast, G. (2004) How did alternative splicing evolve? *Nat. Rev. Genet.*, **5**, 773–782.
- Lear, A.L., Eperon, L.P., Wheatley, I.M. and Eperon, I.C. (1990) Hierarchy for 5' splice site preference determined in vivo. *J. Mol. Biol.*, **211**, 103–115.
- Buratti, E. and Baralle, F.E. (2004) Influence of RNA secondary structure on the pre-mRNA splicing process. *Mol. Cell Biol.*, **24**, 10505–10514.

32. Saliou, J.M., Bourgeois, C.F., Ayadi-Ben, M.L., Ropers, D., Jacquenet, S., Marchand, V., Stevenin, J. and Branlant, C. (2009) Role of RNA structure and protein factors in the control of HIV-1 splicing. *Front Biosci.*, **14**, 2714–2729.
33. Cooper, T.A. and Mattox, W. (1997) The regulation of splice-site selection, and its role in human disease. *Am. J. Hum. Genet.*, **61**, 259–266.
34. Baralle, D. and Baralle, M. (2005) Splicing in action: assessing disease causing sequence changes. *J. Med. Genet.*, **42**, 737–748.
35. Gabut, M., Mine, M., Marsac, C., Brivet, M., Tazi, J. and Soret, J. (2005) The SR protein SC35 is responsible for aberrant splicing of the Elalpha pyruvate dehydrogenase mRNA in a case of mental retardation with lactic acidosis. *Mol. Cell Biol.*, **25**, 3286–3294.
36. Marchand, V., Santerre, M., Aigueperse, C., Fouillen, L., Saliou, J.M., Van Dorsselaer, A., Sanglier-Cianferani, S., Branlant, C. and Motorin, Y. (2011) Identification of protein partners of the human immunodeficiency virus 1 tat/rev exon 3 leads to the discovery of a new HIV-1 splicing regulator, protein hnRNP K. *RNA Biol.*, **8**, 325–342.
37. Maenner, S., Blaud, M., Fouillen, L., Savoye, A., Marchand, V., Dubois, A., Sanglier-Cianferani, S., Van, D.A., Clerc, P., Avner, P. *et al.* (2010) 2-D structure of the A region of Xist RNA and its implication for PRC2 association. *PLoS Biol.*, **8**, e1000276.
38. Zahler, A.M., Lane, W.S., Stolk, J.A. and Roth, M.B. (1992) SR proteins: a conserved family of pre-mRNA splicing factors. *Genes Dev.*, **6**, 837–847.
39. Labourier, E., Allemand, E., Brand, S., Fostier, M., Tazi, J. and Bourbon, H.M. (1999) Recognition of exonic splicing enhancer sequences by the Drosophila splicing repressor RSF1. *Nucleic Acids Res.*, **27**, 2377–2386.
40. Schneider, M., Will, C.L., Anokhina, M., Tazi, J., Urlaub, H. and Luhrmann, R. (2010) Exon definition complexes contain the tri-snRNP and can be directly converted into B-like pre-catalytic splicing complexes. *Mol. Cell*, **38**, 223–235.
41. Kornblihtt, A.R. (2007) Coupling transcription and alternative splicing. *Adv. Exp. Med. Biol.*, **623**, 175–189.
42. Tuduri, S., Crabbe, L., Conti, C., Tourriere, H., Holtgreve-Grez, H., Jauch, A., Pantescio, V., De Vos, J., Thomas, A., Theillet, C. *et al.* (2009) Topoisomerase I suppresses genomic instability by preventing interference between replication and transcription. *Nat. Cell Biol.*, **11**, 1315–1324.
43. Fong, L.G., Vickers, T.A., Farber, E.A., Choi, C., Yun, U.J., Hu, Y., Yang, S.H., Coffinier, C., Lee, R., Yin, L. *et al.* (2009) Activating the synthesis of progerin, the mutant prelamin A in Hutchinson-Gilford progeria syndrome, with antisense oligonucleotides. *Hum. Mol. Genet.*, **18**, 2462–2471.
44. Brunel, C., Marquet, R., Romby, P. and Ehresmann, C. (2002) RNA loop-loop interactions as dynamic functional motifs. *Biochimie*, **84**, 925–944.
45. Hiller, M., Zhang, Z., Backofen, R. and Stamm, S. (2007) Pre-mRNA secondary structures influence exon recognition. *PLoS Genet.*, **3**, e204.
46. Shepard, P.J. and Hertel, K.J. (2008) Conserved RNA secondary structures promote alternative splicing. *RNA*, **14**, 1463–1469.
47. Varani, L., Hasegawa, M., Spillantini, M.G., Smith, M.J., Murrell, J.R., Ghetti, B., Klug, A., Goedert, M. and Varani, G. (1999) Structure of tau exon 10 splicing regulatory element RNA and destabilization by mutations of frontotemporal dementia and parkinsonism linked to chromosome 17. *Proc. Natl Acad. Sci. USA*, **96**, 8229–8234.
48. Grover, A., Houlden, H., Baker, M., Adamson, J., Lewis, J., Prihar, G., Pickering-Brown, S., Duff, K. and Hutton, M. (1999) 5' splice site mutations in tau associated with the inherited dementia FTDP-17 affect a stem-loop structure that regulates alternative splicing of exon 10. *J. Biol. Chem.*, **274**, 15134–15143.
49. Fong, L.G., Ng, J.K., Lammerding, J., Vickers, T.A., Meta, M., Cote, N., Gavino, B., Qiao, X., Chang, S.Y., Young, S.R. *et al.* (2006) Prelamin A and lamin A appear to be dispensable in the nuclear lamina. *J. Clin. Invest.*, **116**, 743–752.
50. Yang, S.H., Qiao, X., Farber, E., Chang, S.Y., Fong, L.G. and Young, S.G. (2008) Eliminating the synthesis of mature lamin A reduces disease phenotypes in mice carrying a Hutchinson-Gilford progeria syndrome allele. *J. Biol. Chem.*, **283**, 7094–7099.
51. Yang, S.H., Bergo, M.O., Toth, J.I., Qiao, X., Hu, Y., Sandoval, S., Meta, M., Bendale, P., Gelb, M.H., Young, S.G. and Fong, L.G. (2005) Blocking protein farnesyltransferase improves nuclear blebbing in mouse fibroblasts with a targeted Hutchinson-Gilford progeria syndrome mutation. *Proc. Natl Acad. Sci. USA*, **102**, 10291–10296.
52. Hua, Y., Sahashi, K., Hung, G., Rigo, F., Passini, M.A., Bennett, C.F. and Kraimer, A.R. (2010) Antisense correction of SMN2 splicing in the CNS rescues necrosis in a type III SMA mouse model. *Genes Dev.*, **24**, 1634–1644.
53. Tazi, J., Durand, S. and Jeanteur, P. (2005) The spliceosome: a novel multi-faceted target for therapy. *Trends Biochem. Sci.*, **30**, 469–478.
54. Scaffidi, P. and Misteli, T. (2005) Reversal of the cellular phenotype in the premature aging disease Hutchinson-Gilford progeria syndrome. *Nat. Med.*, **11**, 440–445.
55. Soret, J., Gabut, M. and Tazi, J. (2006) SR proteins as potential targets for therapy. *Prog. Mol. Subcell. Biol.*, **44**, 65–87.
56. Soret, J., Bakkour, N., Maire, S., Durand, S., Zekri, L., Gabut, M., Fic, W., Divita, G., Rivalle, C., Dauzonne, D. *et al.* (2005) Selective modification of alternative splicing by indole derivatives that target serine-arginine-rich protein splicing factors. *Proc. Natl Acad. Sci. USA*, **102**, 8764–8769.
57. Bakkour, N., Lin, Y.L., Maire, S., Ayadi, L., Mahuteau-Betzer, F., Nguyen, C.H., Mettling, C., Portales, P., Grierson, D., Chabot, B. *et al.* (2007) Small-molecule inhibition of HIV pre-mRNA splicing as a novel antiretroviral therapy to overcome drug resistance. *PLoS Pathog.*, **3**, 1530–1539.
58. Nagy, A., Gertsenstein, M., Vintersten, K. and Behringer, R. (2006) Preparing mouse embryo fibroblasts. *Cold Spring Harb. Protoc.*, doi:10.1101/pdb.prot4398.
59. Durocher, Y., Perret, S. and Kamen, A. (2002) High-level and high-throughput recombinant protein production by transient transfection of suspension-growing human 293-EBNA1 cells. *Nucleic Acids Res.*, **30**, E9.
60. Allemand, E., Gattoni, R., Bourbon, H.M., Stevenin, J., Caceres, J.F., Soret, J. and Tazi, J. (2001) Distinctive features of Drosophila alternative splicing factor RS domain: implication for specific phosphorylation, shuttling, and splicing activation. *Mol. Cell Biol.*, **21**, 1345–1359.
61. Damier, L., Domenjoud, L. and Branlant, C. (1997) The D1-A2 and D2-A2 pairs of splice sites from human immunodeficiency virus type 1 are highly efficient in vitro, in spite of an unusual branch site. *Biochem. Biophys. Res. Commun.*, **237**, 182–187.